NPS ARCHIVE
1960
BERGE, N.

PHOTOELASTIC ANALYSIS OF REINFORCED CIRCULAR HOLES IN PLATES UNDER COMPRESSION

NORMAN K. BERGE
and
JOHN H. SWEENEY

DUDLEY KNOX LIBRARY
NAVAL POSTGRADUATE SCHOOL
MONTEREY CA 93[illegible]3-5101

M3Y

PHOTOELASTIC ANALYSIS OF REINFORCED CIRCULAR HOLES IN PLATES UNDER COMPRESSION

by

NORMAN K. BERGE
Lieutenant, United States Navy
B.S., United States Naval Academy

and

JOHN H. SWEENEY
Lieutenant, United States Navy
B.S., University of North Carolina

SUBMITTED IN PARTIAL FULFILLMENT

OF THE REQUIREMENTS FOR THE

DEGREE OF NAVAL ENGINEER

AND THE DEGREE OF

MASTER OF SCIENCE IN NAVAL ARCHITECTURE

at the

MASSACHUSETTS INSTITUTE OF TECHNOLOGY

May 1960

DUDLEY KNOX LIBRARY
NAVAL POSTGRADUATE SCHOOL
MONTEREY CA 93943-5101

PHOTOELASTIC ANALYSIS OF REINFORCED CIRCULAR HOLES IN PLATES UNDER COMPRESSION by NORMAN K. BERGE and JOHN H. SWEENEY. Submitted to the Department of Naval Architecture and Marine Engineering on 21 May 1960 in partial fulfillment of the requirements for the Master of Science degree in Naval Architecture and Marine Engineering and the Professional degree, Naval Engineer.

ABSTRACT

The purpose of this investigation is to determine the optimum configuration of reinforcement for stress raisers in plates under compression. The stress raisers considered were round holes of approximately three inches in diameter located at the center of one quarter inch thick flat plates. The plates considered are approximately 6" X 6" in size, and were cut from Columbia Resin (CR-39) plastic material.

The investigation was made by applying a uniform load on two edges of the plates and studying the isochromatic pattern in a circular polariscope with dark field. The effect of the various types of reinforcement was studied by using seven different models:

1. Unreinforced plate.
2. Plate with 1/8" circular reinforcement cemented to both sides.
3. Plate with 1/8" circular reinforcement cemented to one side only.
4. Plate with 1/4" circular reinforcement cemented to one side only.
5. Plate with 1/8" square reinforcement cemented to both sides.
6. Plate with 1/8" elliptical reinforcement cemented to both sides with the major axis parallel to the loaded edges.
7. Plate with 1/8" elliptical reinforcement cemented to both sides with the major axis perpendicular to the loaded edges.

Except for model #3, the volume of the material contained in the reinforcement was approximately equal to the volume of the material removed from the original plate to make the hole. Thus the weight of the reinforcement is the same in each case except for model #3.

The point of maximum stress in each model is at the edge of the circular hole on the axis of symmetry which is parallel to the loaded edges. Thus the performance of the reinforcement can be evaluated on

the basis of the stress concentration factor observed at this point. The stress concentration factor is evaluated on the basis of the nominal stress at the same point in an unreinforced model. The models were also observed to determine the load at the inception of buckling.

The unreinforced plate showed a stress concentration factor of 2.70. Model #3 showed a stress concentration factor of 2.25. Models #2, 4, 5, 6 and 7 showed stress concentration factors ranging from 1.66 to 1.76. Models #1, 3 and 4 showed a low resistance bo buckling. Within the limits of experimental error, models #2, 6 and 7 showed approximately the same performance and these were evaluated as the optimum reinforcement configurations. It is concluded that circular or elliptical reinforcement applied to both sides of the stress raiser are the most efficient.

It is recommended that this study be extended by the use of three-dimensional photoelastic analysis to determine the distribution of stress through the thickness of the material. It is further recommended that the investigation be extended to reinforced holes in a cylindrical pressure vessel under external pressure. Some other type of photoelastic material would be required for such an investigation.

Thesis Supervisor: J. Harvey Evans

Title: Associate Professor of Naval Architecture

ACKNOWLEDGEMENT

The authors wish to express their appreciation for the advice and encouragement of Mr. E. E. Johnson of the David Taylor Model Basin, Mr. E. Chapman of Chapman Laboratories, and especially to Professor J. Harvey Evans.

TABLE OF CONTENTS

		Page
	Abstract	i
	Acknowledgement	iii
	Table of Contents	iv
I.	Introduction	1
II.	Procedure	3
III.	Results	4
IV.	Discussion of Results	6
V.	Conclusions	10
VI.	Recommendations	11
VII.	Appendix	
A.	Supplementary Introduction	12
B.	Details of Procedure	14
C.	Summary of Data and Calculations	17
D.	Sample Calculations	18
E.	Supplementary Calculations	21
F.	Original Data	30
G.	Literature Citations	45

1. INTRODUCTION

This thesis is an attempt to show, through photoelastic analysis, the effect of reinforcement around large circular holes in plates under uniform compression. The problem had its foundation in the study of thin-walled cylindrical pressure vessels under uniform external pressure. No analytical solution of the stress distribution around a hole of this sort has yet been published although photoelastic analysis has been used by M. M. Leven (1) to determine stress distributions in thick-walled cylinders using three-dimensional techniques. Specifications of an empirical nature have been written and generally these have proved satisfactory in low pressure installations. The consensus of the various specifications appears to be that an equal amount of material removed to make the hole should be replaced by doubling the thickness around the hole. This reinforcement may be in a circular or an elliptical shape.

Because of the ever increasing pressures to which cylinders are now being subjected, reliance on empirical specifications is in doubt, perhaps even hazardous. However, from a perusal of the literature pertaining to this subject it was found that little investigation has been pursued. Through correspondence with David Taylor Model Basin it was learned that work was in progress, both from analytical and experimental standpoints, but no results were yet available.

These experimental investigations are concerned primarily with three-dimensional analysis. Because of the many complications involved in working with cylindrical shapes, it was

decided to reduce the problem to one of investigating flat plates under uniform compression as a first approximation. This is admittedly an over-simplification of the problem, but with the exception of investigation done by J. B. Mantle with plates in tension (6), little has been accomplished even in this field. Also, the application of edge compression to all four sides and a moment on two opposing sides of the plate simultaneously, which would more nearly approximate the loading conditions in a section cut from a cylinder, was found to be beyond the capability of the existing loading frame which was to be used. Applying uniform compression on two sides of the plate in itself provided considerable difficulty with the equipment available. An advantage of using flat plates is that two-dimensional analysis can be performed which requires no "freezing" of stresses at elevated temperatures and consequently no machining of the models once constructed.

In order to investigate the effect of reinforcement under these conditions six models were machined using CR-39, a plastic resin reported as having good photoelastic properties in compression. One model was unreinforced; the others were constructed with various shaped reinforcements. In all models the nominal dimensions were 6 x 6 inches with a three inch diameter hole in the center. The thickness of the plates was approximately 1/4 inch. The reinforcements were of 1/8 and 1/4 inch material and were cemented to the plates with an epoxy cement. For a more complete description of the models see Appendix B.

II. PROCEDURE

Each model was placed in the loading frame which is described in Appendix B. It was not considered necessary to evaluate the stresses in the entire plate as the regions of primary interest were the axes of the hole perpendicular and parallel to the loading. This obviated the need for determining the isoclinic pattern of the model. Therefore, only the isochromatic pattern was observed in the polariscope using circularly polarized light with a dark field. The pattern was induced by applying uniform pressure along one edge of the plate.

The maximum pressure applied for four of the models was 400 psi. However, the unreinforced plate and the plate with reinforcment of 1/8 inch on one side only tended to buckle at lower pressures. Therefore the maximum pressures used on these plates were 263 and 300 psi respectively, which were below the pressures producing buckling. Photographs were taken at these maximum pressures to be used in the analysis and comparison of the plates. These may be found in Appendix F.

Analytical solutions have been devised for an infinite plate with a small hole (9) and for a plate with a small reinforced hole (7). Comparison of the experimental results and the analytical solution is made in Appendix E. In addition, a compression specimen was machined to determine the fringe constant of the material.

III. RESULTS

The performance of each type of reinforcement is best evaluated by a comparison of the stress concentration factors obtained on each case. This type of comparison is independent of the total load imposed on the model. The comparison is made for the point of maximum stress. This point lies on the edge of the hole on the axis of symmetry of the model which is parallel to the loaded edges (Point 1). The stress concentration factor for each particular model is based on the nominal stress at the same point in a similar unreinforced model.

The stress concentration factors determined for the various models are as follows:

1.	Unreinforced plate	2.70
2.	Plate with 1/8" circular reinforcement onboth sides	1.70
3.	Plate with 1/8" circular reinforcement on one side only	2.25
4.	Plate with 1/4" circular reinforcement on one side only	1.69
5.	Plate with 1/8" square reinforcement on both sides	1.76
6.	Plate with 1/8" elliptical reinforcement on both sides - major axis horizontal	1.72
7.	Plate with 1/8" elliptical reinforcement on both sides - major axis vertical	1.66

Models #1, 3 and 4 showed a tendency to buckle under the compressive loading. The circular and elliptical reinforcements on

both sides of the plate are seen to be the best solution to the problem. The variation in stress concentration factor between the most efficient models, #2, 6 and 7, was small.

Comparing the stress in the unreinforced plate obtained by the theory of Kirsch to that obtained experimentally it was found that the maximum stress determined from the latter was 1.82 times greater than that predicted by theory. Similarly, in the plate with a circular reinforcement on both sides the maximum stress was 1.64 times greater than that predicted by the theory of Levy, et al.

IV. DISCUSSION OF RESULTS

The comparison of the effectiveness of the various reinforcements by means of stress concentration factors makes the investigation independent of the total load applied and the fringe constant. The stress concentration factor can be expected to vary with the ratio of the hole diameter to the total plate width and the ratio of the hole diameter to plating thickness.

Thus the results of this investigation primarily apply to cases where the ratio of hole diameter to plating thickness is:

$$\frac{D}{t} = \frac{3''}{1/4''} = 12$$

and the ratio of the hole diameter to the original intact plate width is:

$$\frac{D}{b} = \frac{3''}{6''} = \frac{1}{2}$$

The sources of error in a photoelastic analysis of this type are numerous and considerable skill is required to obtain precise results. The nature of the CR-39 material is such that its properties change considerably with time, temperature, and moisture content. The moisture content changes according to the humidity of the surrounding atmosphere. The material is also subject to relatively high optical creep.

The machining of models presents considerable difficulty to the inexperienced machinist. Higher accuracy could be obtained with models produced with the aid of a precision milling machine. The models used in this investigation showed some deviation from symmetry and some variation in the $\frac{D}{t}$ and $\frac{D}{b}$ ratios discussed above due to small errors in

machining the models and variations in the thickness of the CR-39 sheets supplied by the manufacturer.

The isochromatic patterns observed in the experiment proved to be fairly symmetrical. An examination of the accompanying photographs will reveal that good symmetry of loading was achieved.

Since CR-39 is an insoluble material, it is impossible to weld the reinforcements to the plates by means of a common solvent. The epoxy cement which was used provided an adequate bond, but the cement that collected at the edge of the joint at the outer periphery of the reinforcement created a small area which was virtually opaque. The exact location of the fringe in this area is impossible.

Another source of difficulty inherent in the photoelastic analysis is the finite width of the fringes. In some cases it was difficult to pick out the exact center of the isochromatic fringe. The stress at the edge of the hole was determined by plotting the $\sigma_1 - \sigma_2$ curves for each model and extrapolating these curves to the edge. The extrapolation process is another source of error.

The qualitative results of this investigation are listed in the previous section.

The models with reinforcements on only one side, models #3 and 4, are considered a poor solution to the problem due to their poor resistance to buckling. The existence of the reinforcement on only one side constitutes a built-in eccentricity which lowers the critical buckling load.

The remaining four models, #2, 5, 6 and 7, all exhibit stress concentration factors of the same magnitude. Model #5, the square rein-

forcement, shows the highest stress concentration in this group, as might be expected. The remaining models, circular and elliptical, are considered the most efficient of those studied. Any one of these four configurations could be used satisfactorily as reinforcements for circular holes if interference problems existed in the structure, but the elliptical configuration is believed to be the most efficient design. In addition, the elliptical reinforcement with the major axis parallel to the load appears to have the least concentration factor of all the models. This is not readily explained logically, however, this narrowing of the reinforcement at the point of maximum stress concentration appears to have a beneficial effect. In the paper by Levy, one conclusion reached is that the reinforcement should be concentrated as close as possible to the hole. This would appear to be substantiated by the results of this analysis.

Within the limits of the design configurations studied, the stress concentration factors developed by this investigation could be used as design criteria. Since the inception of buckling was not reached for the four optimum models, none of these four can be stated to be superior in resistance to buckling on the basis of this investigation.

Further investigation would include the study of models in which the volume of reinforcement material is greater or less than that removed from the intact plate. Such models would employ reinforcements in varying degrees of thickness and of area. It is recommended further that studies be made on reinforced holes in cylindrical and spherical pressure vessels. Because of the problem of forming the normal photoelastic materials this would necessitate the use of cast resins machined to the

configuration desired. These studies should be extended by the use of three-dimensional photoelastic techniques to determine the distribution of stress through the thickness of the material.

It is apparent from the comparison of the theoretical and experimental results in Appendix E that the size of the plate has a pronounced effect on the stress concentration. Both the theories for flat plates with small holes are based on an infinite plate and experimental results using very large plates agree within a few percent. However, using small plates with large holes introduces considerably greater error.

V. CONCLUSIONS

This investigation indicates that the best type of reinforcement for a round hole in a plate under compression is a round or elliptical collar with an equal amount of reinforcement material on each side of the plate. The reinforcements studied contained approximately the same volume of material that was removed from the intact plate to make the hole, but is not considered to be the only solution. The volume of material, and hence thickness, would depend primarily on the severity of loading.

The reinforcements which were applied to only one side of the plates gave a low resistance to buckling and are considered inefficient.

The best performing reinforcements resulted in a decrease in the stress concentration factor from 2.70 in the unreinforced plate to the order of 1.75 in the optimum reinforced plates. The highest stress concentration occurs at the edge of the hole on the axis of symmetry of the model which is parallel to the loaded edges. This is a compressive stress.

It is not possible to determine the stress concentration at the edge of the hole by the theories developed to date unless the plate is very large. For small plates it is necessary to determine the stress concentration experimentally.

VII. APPENDIX

VI. RECOMMENDATIONS

The results of this investigation indicate that further work along the same lines would be beneficial. Models should be constructed with reinforcements of volume greater than or less than that of the material removed from the intact plate. The reinforcement thickness should vary in relation to the thickness of the basic plating.

A study of models with varying ratios of hole diameters to plating width would be helpful. Interaction of stresses around two or more closely spaced holes could also be studied.

Three-dimensional photoelastic techniques could be employed to determine the distribution of stresses through the thickness of the plating. This method could also be used to investigate the stress concentrations around holes in cylindrical pressure vessels.

The use of CR-39 is recommended for use in flat plate form only. It softens only slightly at increased temperature and can not be formed without inducing high residual stresses. The use of cast resins machined to the desired configuration is recommended for cylinders. This method has been used with excellent results in the study of thick-walled cylinders and will probably yield good results for thin-walled, stiffened cylinders also.

Since it has been shown that theoretical analysis will not yield good results for finite plates with large holes it is recommended that photoelastic analysis be used to examine models of the desired structure whenever there is any doubt as to the degree of reinforcement required. The initial cost of the equipment is high; but the cost of the photoelastic material is not unreasonable, and the end result of a safer structure would more than justify the expenditure.

A. SUPPLEMENTARY INTRODUCTION

At the outset of this investigation it was desired that a study be made of the stress concentrations around holes in cylindrical pressure vessels. It was hoped that thin-walled cylinders of photoelastic material could be purchased in the manufactured state. It was found that cylinders of the size desired (about ten inches diameter) were unavailable, although it was possible to obtain smaller diameters. However, smaller diameters would not be satisfactory as the wall thickness to diameter ratios were such as to classify the cylinders as thick-walled.

As an alternative, the possibility of using cast resins machined to the desired configuration was investigated. This showed some promise as the process has been imminently successful for three-dimensional analysis of thick-walled cylinders. However, the cost was prohibitive for an investigation of this sort using limited funds. Therefore, it was decided to investigate simple flat plates with large holes as stress raisers and it was found that little had been accomplished with finite plates. In large plates with small holes St. Venant's principle regarding the effect of the stress concentration being negligible far from the hole is valid, but the effect of reducing the size of the plate had not been explored thoroughly.

Since relatively thin plates were to be used with various reinforcements, it was not considered necessary to use three-dimensional analysis. The regions of primary interest are the stress concentrations at the hole. No attempt was made to chamfer the outer edge of the reinforcement as is done in actual practice to insure smooth transitions of the stress distribution. This was not the object of the study, but if it

were to be investigated, three-dimensional analysis would be indicated.

Two-dimensional photoelastic techniques permit a much more rapid means of determining stress distributions. The models may be examined under any desired degree of loading within the capability of the loading frame. The object of this investigation was primarily the comparison of various shapes of reinforcement around circular holes, hence the models were subjected to the same loading where possible. No buckling calculations were made for the models, but it was recognized as a distinct possibility. Therefore, care was taken not to precipitate buckling.

The analysis was further simplified because it was only necessary to examine the stress concentrations, and of course these occurred at the edge of the hole on the axes parallel and perpendicular to the load. The direct calculation using the applied load, the order of the fringe, and the fringe constant of the material yields $\sigma_1 - \sigma_2$. At the edge of the hole σ_2 equals zero and therefore the σ_1 stresses for the various plates may be compared immediately. In this way it was hoped that an optimum configuration of reinforcement could be obtained.

A secondary purpose of this investigation was to examine the effect of varying the thickness of reinforcement and also the disposition. For this reason models were constructed with reinforcement on one side only and of two different thicknesses. This configuration was decided upon because of limitations in material thicknesses which could be supplied and in order to examine the effect of unsymmetrical transverse reinforcement.

B - DETAILS OF PROCEDURE

Photoelastic models for this investigation were constructed of cemented laminar sheets of CR 39. Sheets were first rough cut to shape with a small hand-held electric jig saw and then finished with Chapman "Photoelastic Model Maker," which is a high speed rotary cutter. Aluminum templates were attached to the CR 39 sheets to provide a guide for the rotary cutter. The cutter produces a smooth, even surface which is relatively free of machining stresses. The high tool speed and small depth of cut make it possible to avoid the development of excessive heat at the model surface.

The models consisted of an essentially square plate approximately 6" x 6" with a central circular hole of approximately 3" diameter. Reinforcements of various shapes from 1/8" and 1/4" CR 39 sheet were cemented to one or both sides of the square plates. Dimensions of the various models vary slightly due to errors in the templates and machining errors.

The reinforcements were cemented to the square plates by means of an epoxy obtained from the supplier of the CR 39 material (Chapman Laboratories). It was necessary to use an epoxy cement because the CR 39 material is insoluble and cannot be welded in the conventional methods of joining plastics. The cement is transparent and has mechanical properties close to those of CR 39. It is apparent from the photographs that some difficulty was experienced with cement seeping out between the joints on the surface of the model. This is a minor problem since the area affected is very small.

The method of compressing the completed models is shown in Figure I. The lower edge of the plate fits into a channel cut into the edge of the

bottom support. This channel contains a rubber hose which can be inflated by means of a conventional hydraulic pump. Since the inflation of the pressure hose is restricted by the channel walls and the lower edge of the plate, pressures of the order of 400 psi were obtained without difficulty. The top edge of the plate abutted against the upper support which was cushioned by a pdece of soft rubber. This method of compressing the edges of the plate provided a uniform distribution of the load as shown in the accompanying photographs (Appendix F).

The pressure on the system was determined by the use of an ordinary 1000 psi Bourdon gage. The maximum load obtained was limited by the buckling strength of the particular model being investigated. One photograph was taken of each model in its condition of maximum load. The plates were not loaded to the limiting buckling value in order to avoid permanent deformation of the model.

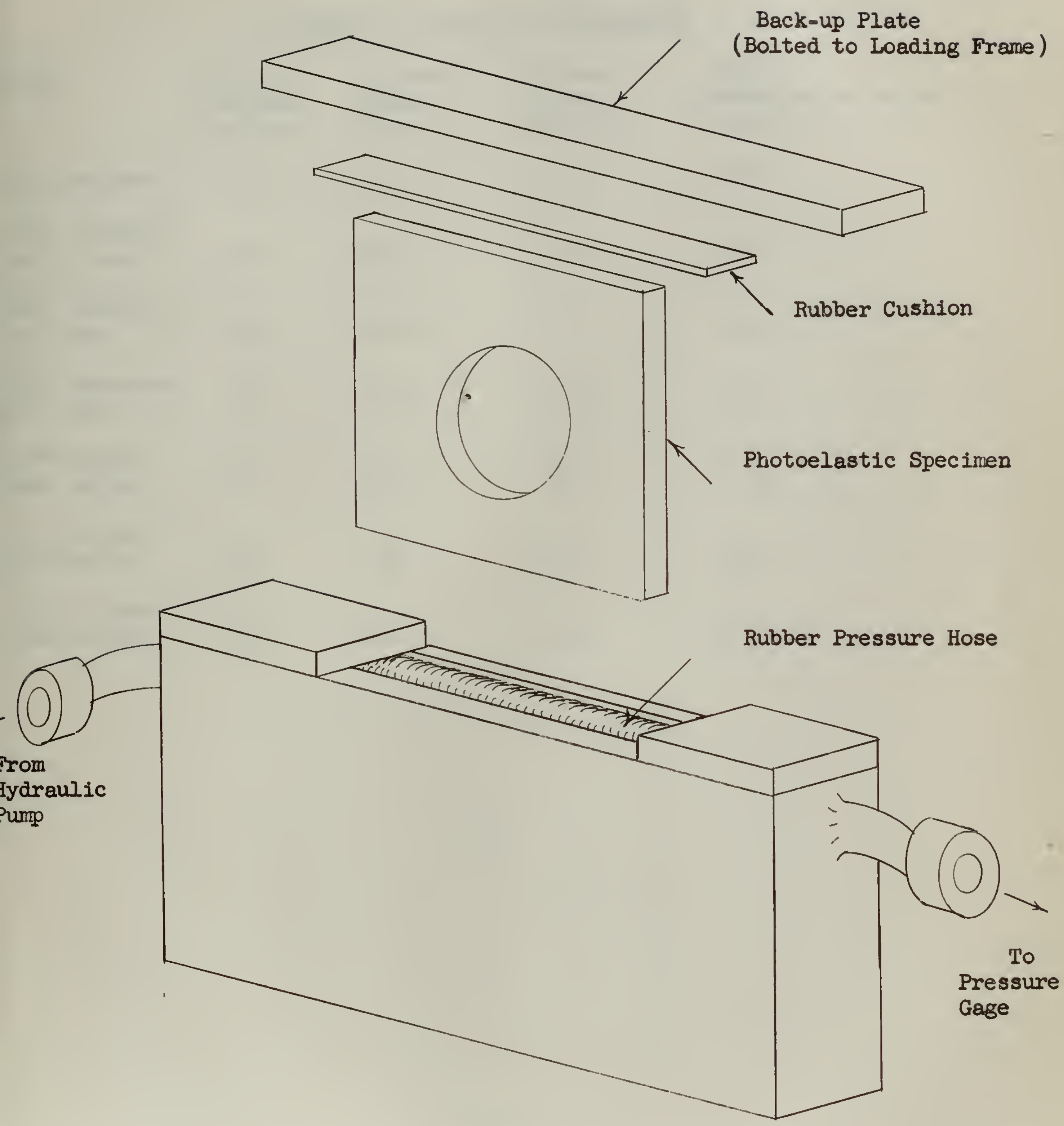

FIGURE I.

Exploded View of Loading Device

NKB
5/60

C. SUMMARY OF DATA AND CALCULATIONS

Model	Maximum Pressure Applied	Maximum Stress Point 1	Maximum Stress Point 2	Stress Concentration Factor Point 1
1. Unreinforced	263	1435	1120	2.70
2. 1/8" circular both sides	400	1460	830	1.70
3. 1/8" circular one side	300	1380	770	2.25
4. 1/4" circular one side	400	1450	930	1.69
5. 1/8" square both sides	400	1400	735	1.76
6. 1/8" ellipse both sides	400	1380	910	1.72
7. 1/8" ellipse both sides	400	1310	620	1.66

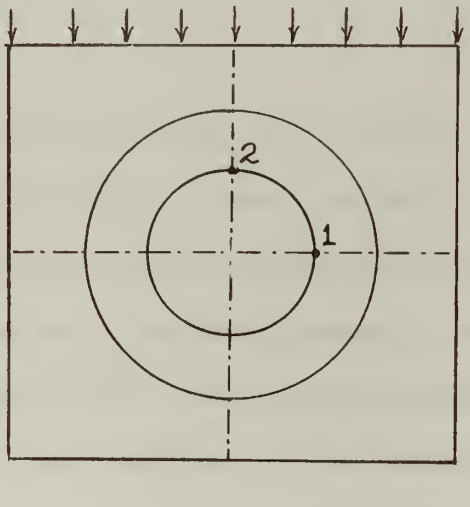

D. SAMPLE CALCULATIONS

Calculations for Model #2, plate with 1/8" circular reinforcement cemented to both sides of the model:

Volume of material removed from intact plate:

$$V_h = \pi r_1^2 h_1 = \pi (1.5)^2 (.25) = 1.768 \text{ in}^3$$

Size of reinforcement:

$$V_r = 1.768 = V_h$$

$$V_r = \pi r_2^2 h_2 - \pi r_1^2 h_1 = \pi r_2^2 h_2 - 1.768$$

$$\pi r_2^2 (2 \times .125) = (2 \times 1.768)$$

$$r_2^2 = \frac{1.768}{(.125)\pi} = 4.5$$

$$r_2 = 2.121 \text{ in}$$

$$D_2 = 4.24 \text{ in}$$

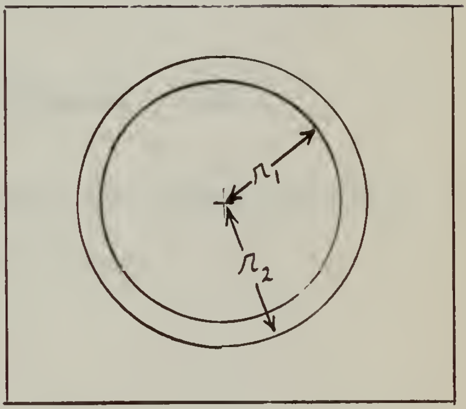

Thus the reinforcing rings have an inside diameter of 3 inches, an outside diameter of 4.24 inches, and are each 1/8" thick.

In the particular model being discussed the actual dimensions differed from the nominal dimensions because of variation in the plate thickness and machining errors. The average thickness of the basic plate was .251 inch; the average thickness of the assembled reinforcement was .510 inch (this figure includes the thickness of the basic plate).

The maximum pressure applied to this model was 400 psi. The inception of fringe orders at the point of maximum stress occurred at the following pressures:

Order	Pressure, psi.
0	0
1	98
2	154
3	193
4	243
5	273
6	315
7	353
8	382

The length of the loaded edge was 5.85 inches. Thus the total load applied was:

$$P = (\text{pressure}) \times (\text{length}) \times (\text{thickness}) = 587 \text{ lb}$$

The nominal stress which would appear across the intact portion of a similar unreinforced plate is calculated as follows:

$$\frac{P}{A} = \frac{587}{(2)(1.36)(.251)} = 860 = \sigma_n$$

Fringe constant = f = 82

h = thickness of material

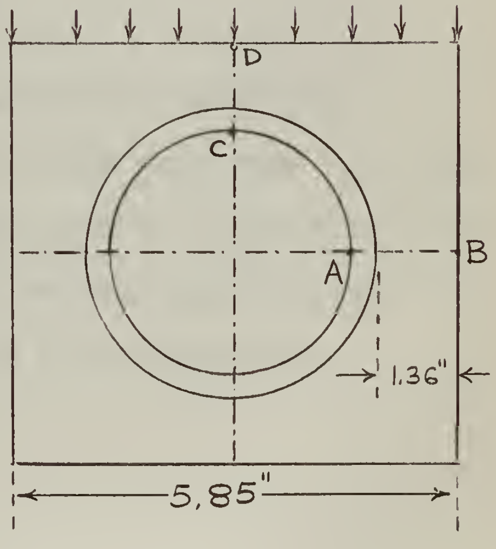

The distribution of orders in the fully loaded model was as follows:

Along line AB

Order n	Distance from A (in)	Material thickness (in) h	Stress $\sigma = \frac{fn}{h}$
8	.060	1/2	1288
7	.106	1/2	1126
6	.166	1/2	966
5	.227	1/2	805
4	.302	1/2	644
3	.393	1/2	483
2	.488	1/2	322
1	.755	1/4	327
0	1.056	1/4	0

These values were plotted on a curve of stress versus distance from A, and the curve was extrapolated to point A on the edge of the hole. The maximum stress, σ_{max}, was read at this point and used to calculate the stress concentration factor of the model.

$$\text{Stress concentration factor} = \frac{\sigma_{max}}{\sigma_n}$$

$$\sigma_{max} = 1460$$

$$\text{SCF} = \frac{1460}{860} = 1.70$$

The distribution of stress along the vertical line CD was also observed and plotted. The curves included in this paper show $\frac{\sigma_1 - \sigma_2}{\sigma_m}$ as a function of percentage of the distance from A to B and from C to D. Since point A is on the free boundary of the inner edge, σ_2 isequal to zero and σ_1 may be read directly from the curve at this point.

E. SUPPLEMENTARY DISCUSSION

Photoelastic Theory

Stress analysis by means of the photoelastic effect is based on these two principles:

1. Light which is incident normal to the surface of a flat plate (photoelastic model) subjected to plane stress within the elastic limit is polarized in the directions of the principal stress axes and is transmitted only on these planes;
2. The velocity of transmission of this light in each principal plane is dependent on the intensities of the principal stresses in these two planes.

Let t_1 and t_2 be the times required for the transmission of light on the two principal planes. Let p be a proportionality factor dependent on the velocity of the light. Then $p(t_1-t_2)$ is the phase difference between the light waves emerging from a photoelastic model. It can be shown that

$$p(t_1-t_2) = P\frac{hc}{v}\left(\sigma_1 - \sigma_2\right)$$

where $(\sigma_1 - \sigma_2)$ is the difference between the principal stresses, h is the thickness of the material, and $\frac{c}{V}$ is the optical constant of the material and the surrounding medium.

Then the phase difference is directly proportional to the difference between the principal stresses, and any method which will indicate the phase difference can be used to determine the value $(\sigma_1 - \sigma_2)$.

The polariscope provides a means of locating points in a flat plate where the value of $(\sigma_1 - \sigma_2)$ is a constant. The plane polariscope consists of a light source, a polarizer, an analyzer, a lens system, and a viewing screen. The photoelastic model is placed in a loading frame between the polarizer and analyzer.

The resultant amplitude of the light wave emerging from the analyzer can be shown to be

$$A = a \sin 2\alpha \left[\sin p\left(\frac{t_1 - t_2}{2}\right)\right] \sin p\left(t - \frac{t_1 + t_2}{2}\right),$$

where α is the angle between the original plane of vibration and the number 1 principal plane.

The intensity of light transmitted through any particular point in the model is proportional to A^2. A dark spot will be observed for each point where

$$\sin p\left(\frac{t_1 - t_2}{2}\right) = 0.$$

These dark spots form the loci of constant value of $(\sigma_1 - \sigma_2)$ and are called isochromatics. Isochromatics are then also loci of points where

$$p\left(\frac{t_1 - t_2}{2}\right) = n\pi.$$

n is an integer

The points where $\sin 2\alpha = 0$ form the loci of constant stress direction (isoclinics).

The plane polariscope is converted to a circular polariscope by the addition of quarter wave plates on either side of the photoelastic model. The quarter wave plates eliminate the isoclinics from the photoelastic stress pattern leaving only the isochromatics which are independent of the stress direction. The circular polariscope indicates the difference between the principal stresses at every point and the actual values of the individual stresses at any free boundary (σ_2 must equal zero at a free boundary).

The difference between the two principal stresses is determined quantitatively by the relation

$$(\sigma_1 - \sigma_2) = \frac{f}{h} \times n$$

where f is the "fringe constant" of the material, n is the order of interference, and h is the thickness of the model.

The isochromatic diagrams obtained on the viewing screen of the circular polariscope give no indication of the actual values of $(\sigma_1 - \sigma_2)$. The values of n must be determined for each point investigated and the value of f must be determined for the particular material used.

DETERMINATION OF THE FRINGE ORDER

This investigation was made using a mercury light source with a green filter. The isochromatic pattern was composed of dark lines on a green field. The fringe orders were determined by locating the zero order fringes and by counting fringes as they passed through a particular point.

The zero order fringe is located by its fixed position. In the dark field polariscope as used, the entire model is covered with the zero order in the unloaded state. When the model is loaded, only the zero order points remain dark. All the other points in the model will vary in brightness as the load changes, but the zero order fringe remains dark.

The order at any particular point may be determined by counting the fringes which pass through the point from the condition of no load to full load. The combined processes of counting orders and locating points of zero order were sufficient to determine the order of every fringe shown by the models.

FRINGE CONSTANT

In order to get the numerical value of the difference between the principal stresses, $\sigma_1 - \sigma_2$, it is necessary to find the value of the "fringe constant," f. The fringe constant is the stress-optic constant for the material. It is the change in the value of $\sigma_1 - \sigma_2$ that will produce a unit change in order of interference fringe at a particular point in a

model of unit thickness. The fringe constant is given by the following equation:

$$f = \frac{(\sigma_1 - \sigma_2) h}{n} \quad \text{lb/inch/order.}$$

A constant value of the fringe constant can be used only in materials where the stress and the optical retardation effect are linearly related. As discussed elsewhere in this paper, CR 39 exhibits this linear relation over the range of stresses which was investigated.

The value of the fringe constant can be determined by observing the interference fringes at any point in any model where the stress can be accurately determined by other than photoelastic methods. Specimens in pure bending, tension, or compression are normally used for calibration.

A simple compression specimen was employed in this investigation for the determination of the fringe constant.

PROPERTIES OF CR-39

The material used in this investigation is a product of the Columbia Chemical Division of the Pittsburgh Plate Glass Company called Columbia Resin, CR 39 and chemically termed allyl diglycol carbonate. It is one of the thermosetting synthetic resins.

The manufacturing process involves the reaction of phosgene with diethylene glycol to obtain a chloroformate which is then esterified with allyl alcohol to produce the diglycol carbonate monomer. The polmerization of this monomer is then effected by heating it in the presence of a catalyst such as benzoyl peroxide. The sheet form is usually obtained by casting it between sheets of plate glass. The finished product has a high optical clarity, is strong and hard, and is infusible and insoluble.

The manufacturer lists the mechanical properties of CR 39 as follows:

Hardness, Rockwell (M-scale)	95-100
Impact Strength @ 25° C (ft-lb/in)	
Izod, notched	0.3-0.4
Izod, unnotched	2-3
Charpy, notched	0.3-0.4
Charpy, unnotched	3-4

It is obvious that this material is relatively brittle compared to the other well-known plastics. The material chips very easily but is otherwise relatively easy to work.

Coolidge(4) found the stress-strain curve for CR 39 to be a straight line to about 3000 psi, with a decreasing modulus of elasticity at higher loadings. The modulus of elasticity was found to be approximately 250,000 psi for loadings less than 3000 psi. The tensile strength was found to vary from 4000 psi to 9000 psi depending on the relative humidity and the time of loading. Higher humidity appears to have a weakening effect on this material.

Annealing of CR 39 seems to have little or no effect on its strength. Excessive temperature will cause deterioration of the plastic. Temperatures of 120° C. should not be exceeded in treating the material.

CR 39 seems to absorb or to lose moisture according to the humidity of the surrounding atmosphere. Coolidge found a marked change in weight in specimens left in the laboratory over a period of time. The storage of CR 39 in either a dry or humid atmosphere does not seem to alter the growth of the edge effect. Material which has been exposed to a dry atmosphere for extended periods becomes increasingly brittle and is difficult to work.

Optical creep is relatively high in CR 39 but this does not make it unsuitable for investigations of relative stress within a specimen.

As stated elsewhere, the fringe constant for this material was found to be 82 lb/in/order. This value was determined by use of a compression calibration specimen. Coolidge found the stress-fringe relationship to be essentially linear up to approximately 3000 psi. The stress-optical coefficient cannot be considered constant because of the high optical creep. Coolidge's value for the fringe constant was about 80.5.

Investigations of the suitability of CR 39 for three-dimensional photoelastic analyses shows that the material suffers from a large decrease in strength at elevated temperatures (110°C.). The necessity of limiting loads to small values at high temperatures will allow only difficult and inaccurate measurements to be made. The frozen stress patterns have also been found to change rapidly with time. This would tend to limit its use for three-dimensional work as the relaxation of the stress patterns during the slicing process would introduce further inaccuracies.

COMPARISON OF THEORETICAL AND EXPERIMENTAL RESULTS

The formulae given in Timoshenko and Goodier(9) as derived by Kirsch for an unreinforced infinite plate with a small hole are as follows:

$$\sigma_r = \frac{S}{2}\left(1 - \frac{a^2}{r^2}\right) + \frac{S}{2}\left(1 + \frac{3a^4}{r^4} - \frac{4a^2}{r^2}\right)\cos 2\theta$$

$$\sigma_\theta = \frac{S}{2}\left(1 + \frac{a^2}{r^2}\right) - \frac{S}{2}\left(1 + \frac{3a^4}{r^4}\right)\cos 2\theta$$

$$\tau_{r\theta} = -\frac{S}{2}\left(1 - \frac{3a^4}{r^4} + \frac{2a^2}{r^2}\right)\sin 2\theta$$

where: S = uniform tension or compression (psi)
a = radius of the hole (in)
r = radius of the point in question from center of the hole (in)
θ = radial angle measured from axis of the hole parallel to the load

As a comparison, the solution to these equations for $\theta = 90^\circ$ (maximum stress cencentration) is presented below and compared to the ecperimental values obtained.

Order	r	σ_r	σ_θ	$(\sigma_\theta - \sigma_r)$	$(\sigma_1 - \sigma_2)$
Edge of hole	1.50	0	-789	-789	-1435
4	1.60	-43	-662	-619	-1260
3	1.73	-74	-582	-508	- 945
2	1.92	-94	-490	-396	- 630
1	2.35	-95	-382	-287	- 315
0	2.87	-79	-328	-249	0
Edge of plate	2.93	-76	-324	-248	+ 30

$S = 263$ psi; $\tau_{r\theta} = 0$; $\sigma_1 = \sigma_\theta$; $\sigma_2 = \sigma_r$

As can be seen, the effect of a large hole in a small plate almost doubles the stress difference predicted by theory. There can be no correlation between the small plate and the infinite plate at radii near the edge of the small plate.

Modification of these formulae was done by S. Levy, et al,(7)

for a circular reinforcement of a small hole in a large plate and are given by:

$$\sigma_r = S\left\{F + K\frac{a^2}{r^2} + \cos 2\theta\left[-A - 3C\frac{a^4}{r^4} - 2D\frac{a^2}{r^2}\right]\right\}$$

$$\sigma_\theta = S\left\{F - K\frac{a^2}{r^2} + \cos 2\theta\left[A + 6B\frac{r^2}{a^2} + 3C\frac{a^4}{r^4}\right]\right\}$$

$$\tau_{r\theta} = S\sin 2\theta\left(A + 3B\frac{r^2}{a^2} - 3C\frac{a^4}{r^4} - D\frac{a^2}{r^2}\right)$$

The constants are determined by using graphs computed for the volume ratio given as follows:

$$\text{Volume Ratio} = \left(\frac{T}{t} - 1\right)\left(\frac{b^2}{a^2} - 1\right)$$

where:
T = thickness of reinforced portion
t = thickness of unreinforced portion
a = diameter of the hole
b = diameter of the reinforcement

For the plate with 1/8" reinforcement on both sides,

Volume ratio = .992 and $\frac{b}{a}$ = 1.401.

Evaluating the constants the following equations result:

Reinforced portion

$$\sigma_r = S\left\{.39 - .39\frac{a^2}{r^2} - \left[.47 + 1.17\frac{a^4}{r^4} - 1.66\frac{a^2}{r^2}\right]\right\}$$

$$\sigma_\theta = S\left\{.39 + .39\frac{a^2}{r^2} - \left[-.47 + .18\frac{r^2}{a^2} - 1.17\frac{a^4}{r^4}\right]\right\}$$

Unreinforced portion

$$\sigma_r = S\left\{.5 - .24\frac{a^2}{r^2} - \left[.5 - .06\frac{a^4}{r^4} - 1.26\frac{a^2}{r^4}\right]\right\}$$

$$\sigma_\theta = S\left\{.5 + .24\frac{a^2}{r^2} - \left[-.5 + .06\frac{a^4}{r^4}\right]\right\}$$

Solution of these results in the following:

Order	r	σ_r	σ_θ	$(\sigma_\theta - \sigma_r)$	$(\sigma_1 - \sigma_2)$
Edge of hole	1.50	0	-896	-896	-1470
8	1.56	-25	-850	-825	-1288
7	1.606	-53	-758	-705	-1126
6	1.666	-73	-691	-618	- 966
5	1.727	-82	-648	-566	- 805
4	1.802	-94	-574	-480	- 644
3	1.893	-102	-517	-415	- 483
2	1.988	-110	-452	-342	- 322
1	2.255	-188	-435	-247	- 327
0	2.556	-183	-430	-247	0
Edge of plate	2.922	-109	-384	-275	+ 270

S 400 psi; $\tau_{r\theta} = 0$

Again there is no correlation between the theoretical and experimental stress differences.

F. ORIGINAL DATA

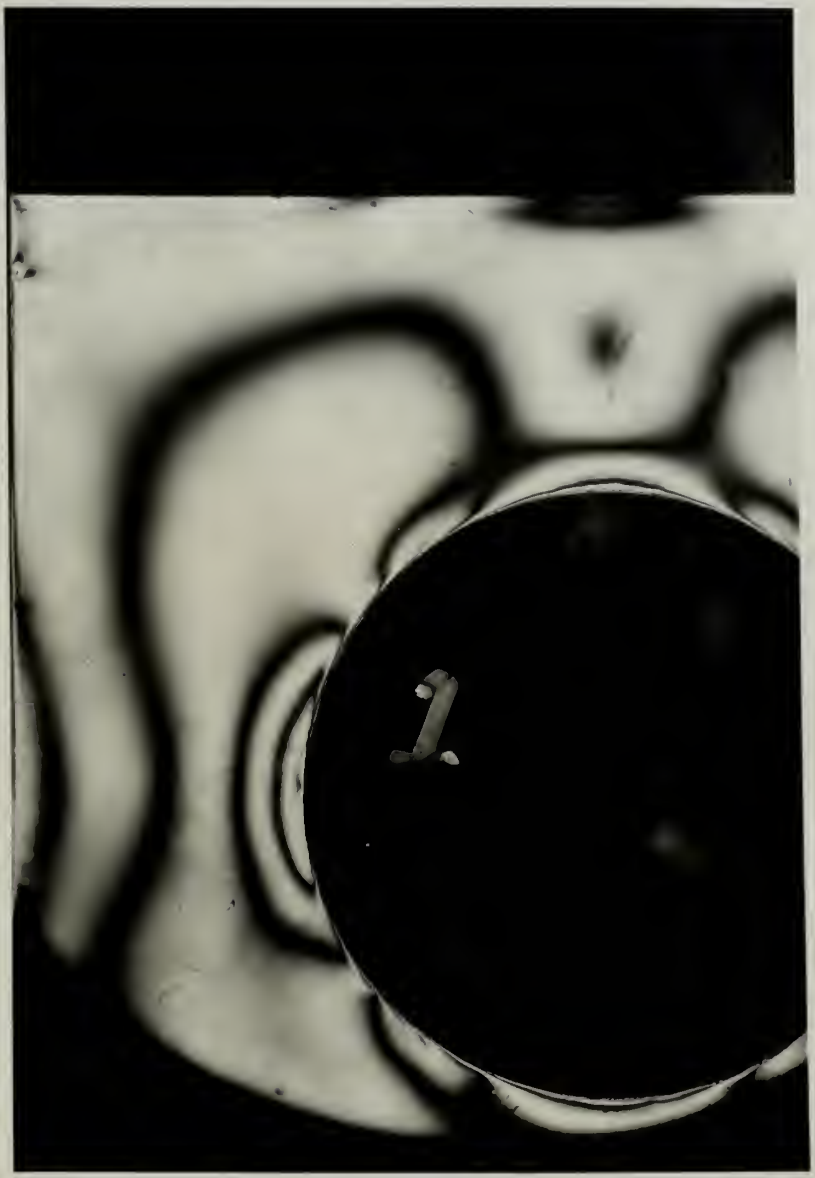

FIGURE II. Unreinforced Plate

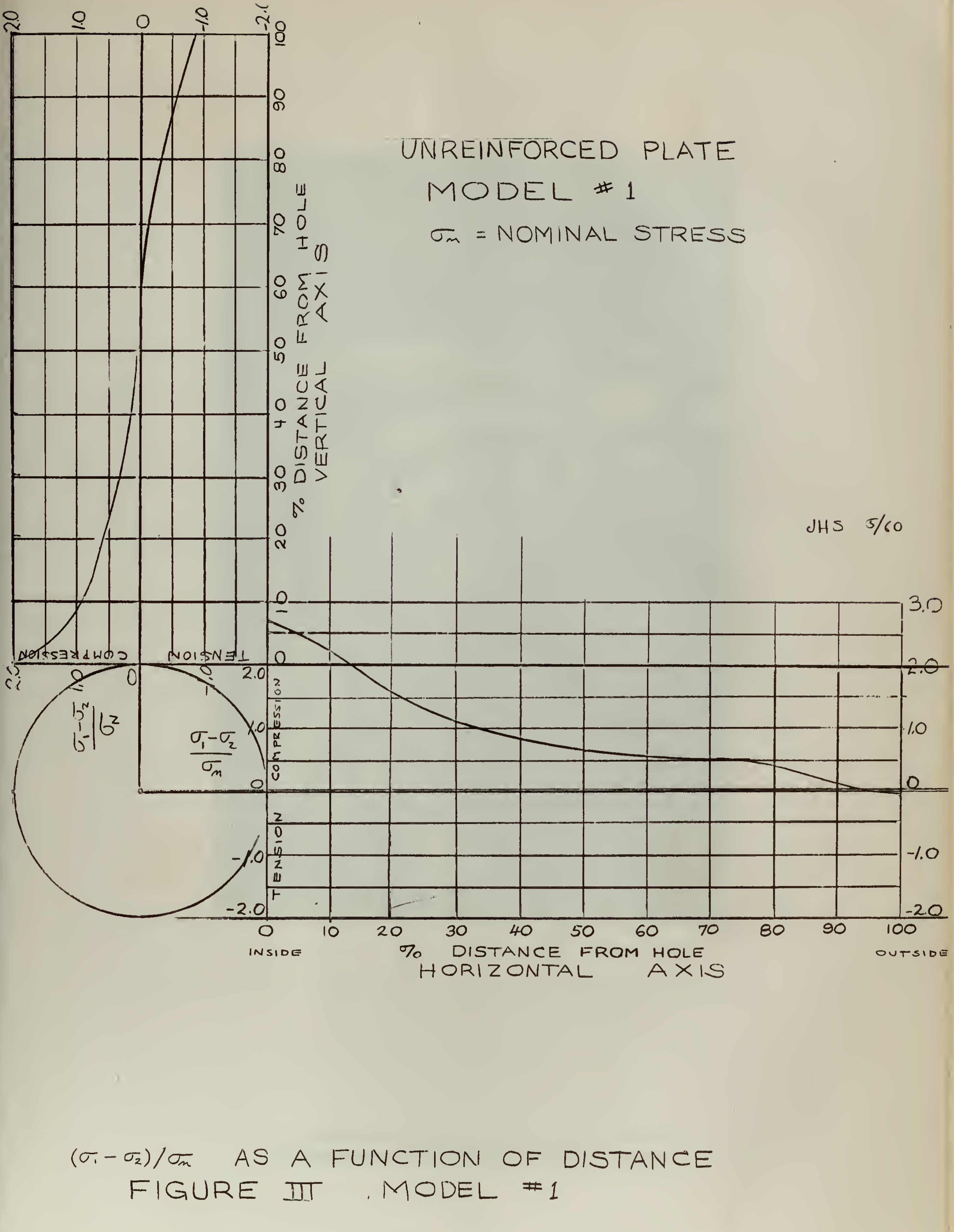

$(\sigma_1 - \sigma_2)/\sigma_m$ AS A FUNCTION OF DISTANCE

FIGURE III . MODEL #1

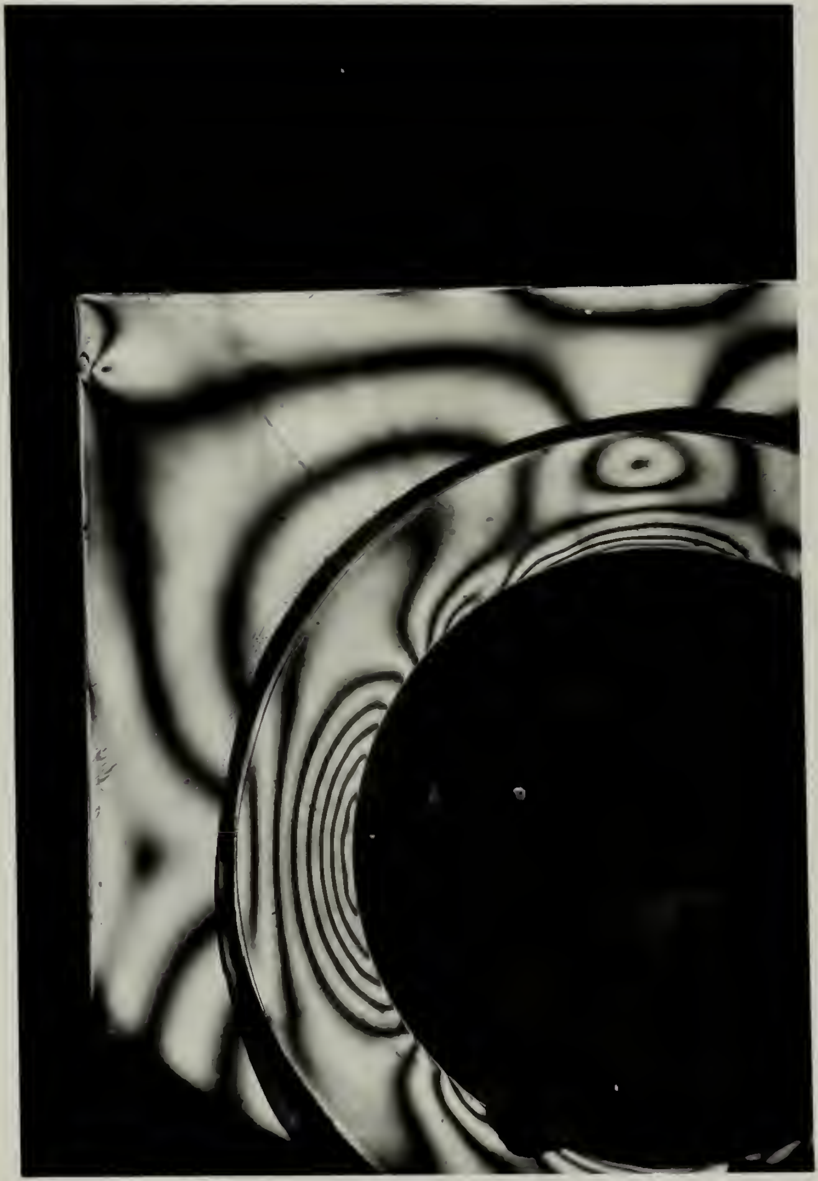

FIGURE IV. Plate with 1/8" Circular Reinforcement Cemented to both Sides

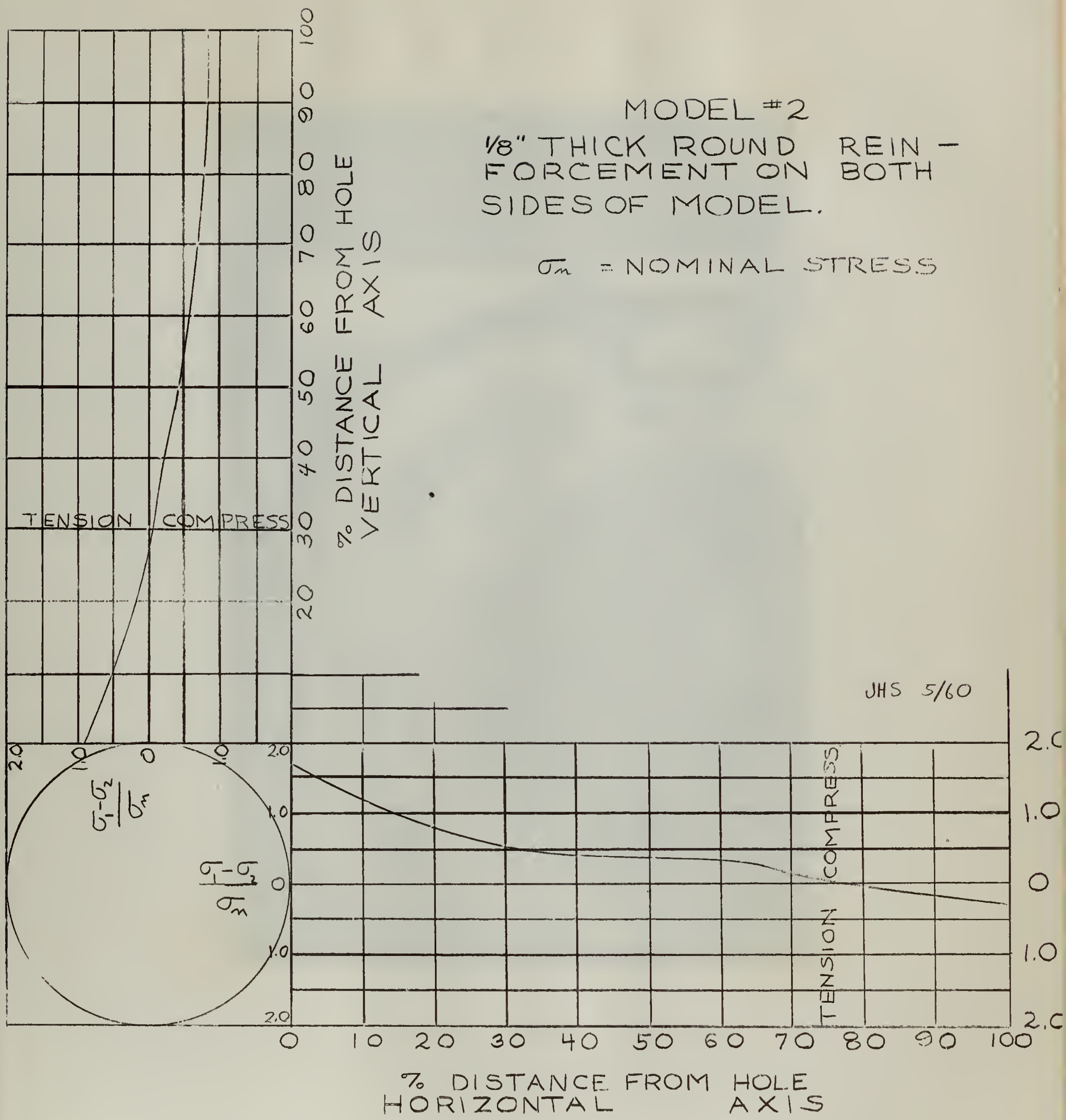

$(\sigma_1-\sigma_2)/\sigma_n$ AS A FUNCTION OF DISTANCE

FIGURE V , MODEL #2

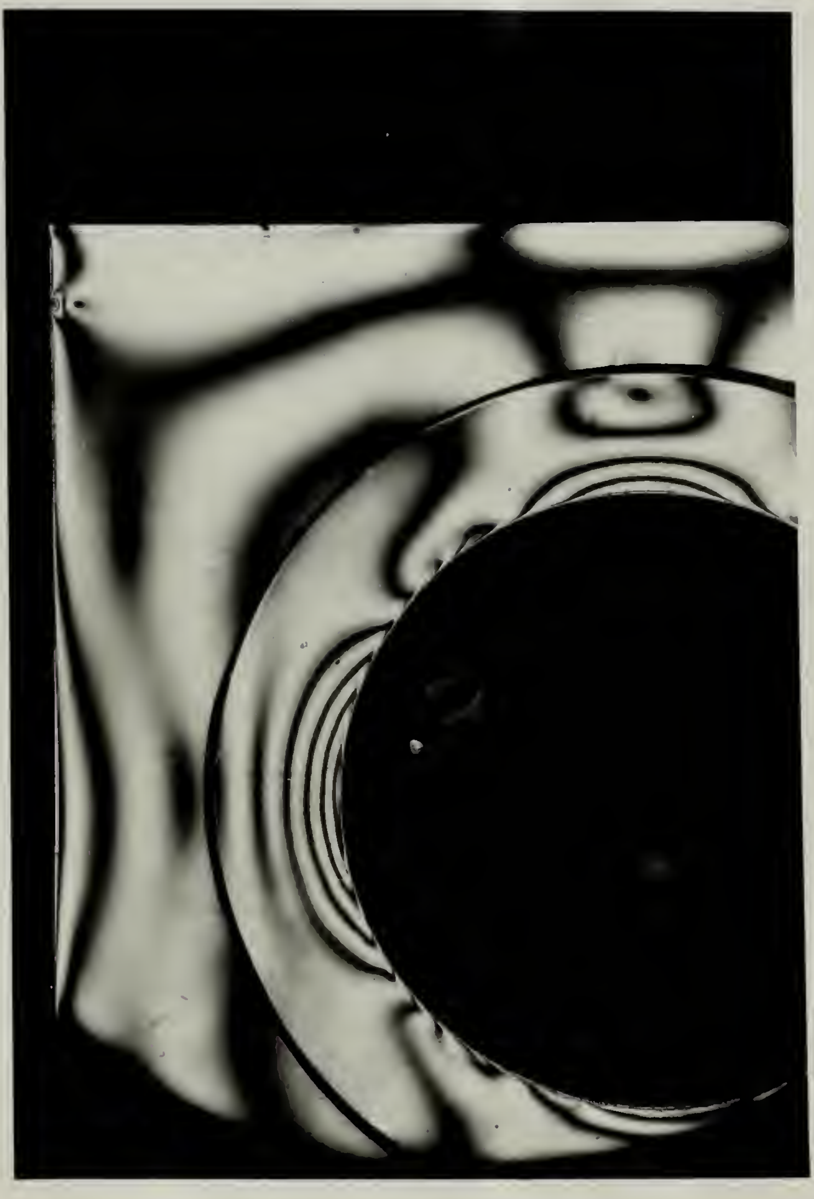

FIGURE VI. Plate with 1/8" Circular Reinforcement Cemented to one Side only

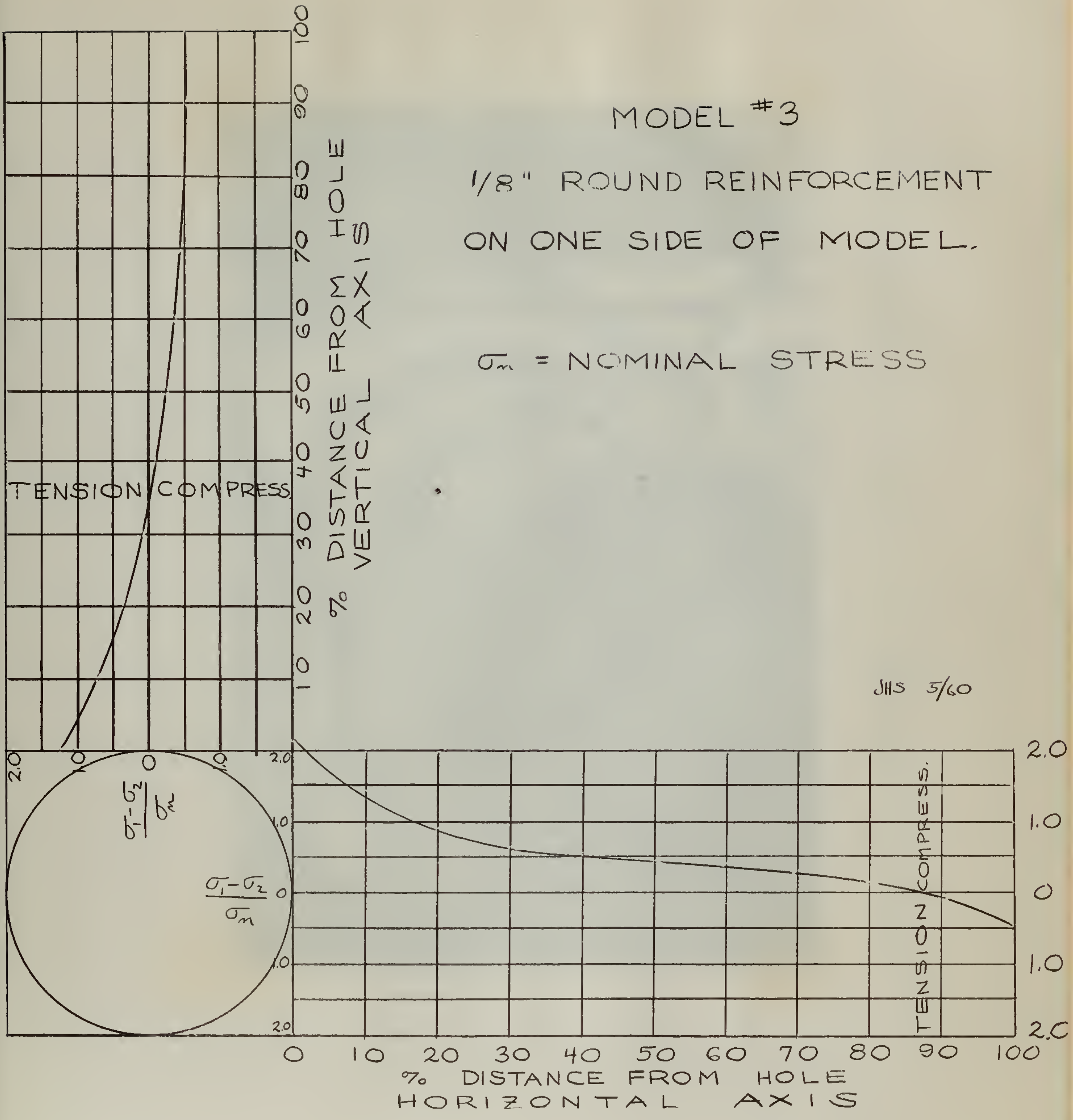

MODEL #3

1/8" ROUND REINFORCEMENT ON ONE SIDE OF MODEL.

σ_m = NOMINAL STRESS

JHS 5/60

$(\sigma_1-\sigma_2)/\sigma_m$ AS A FUNCTION OF DISTANCE

FIGURE VII . MODEL #3

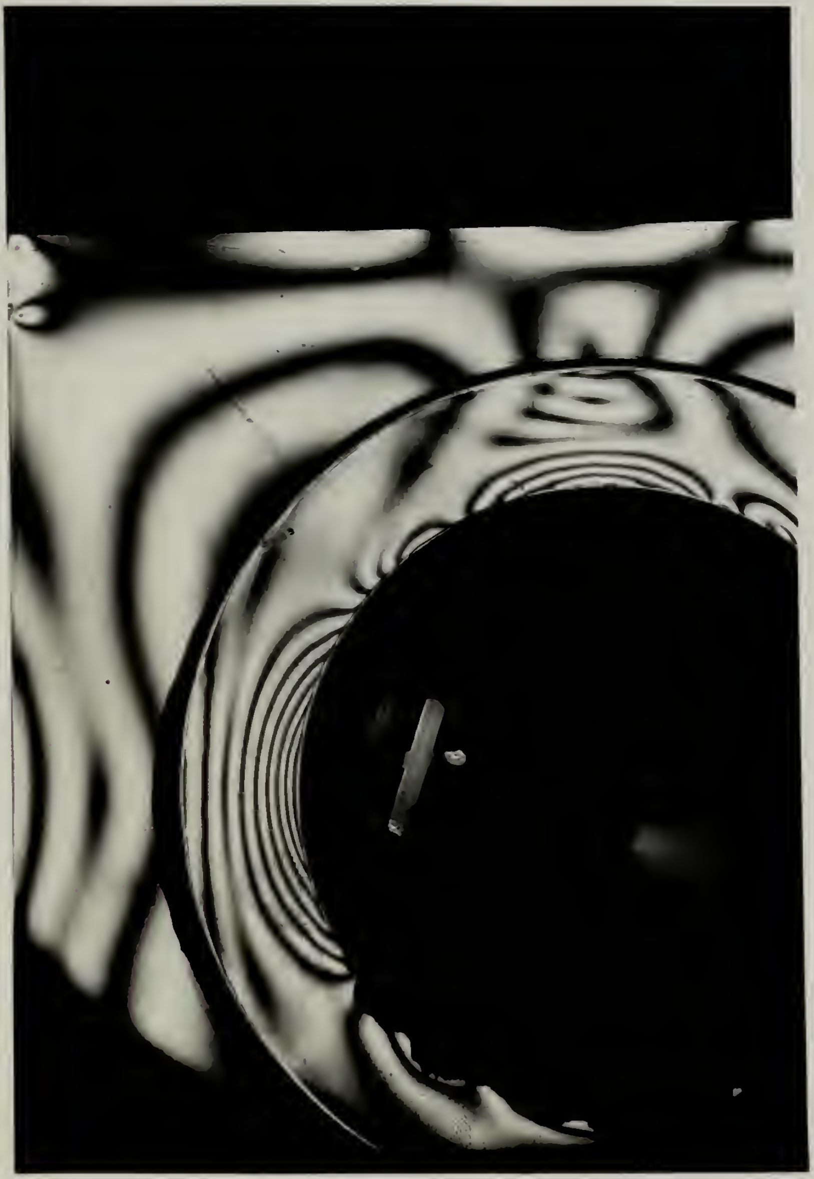

FIGURE VIII. Plate with 1/4" Circular Reinforcement Cemented to One Side only

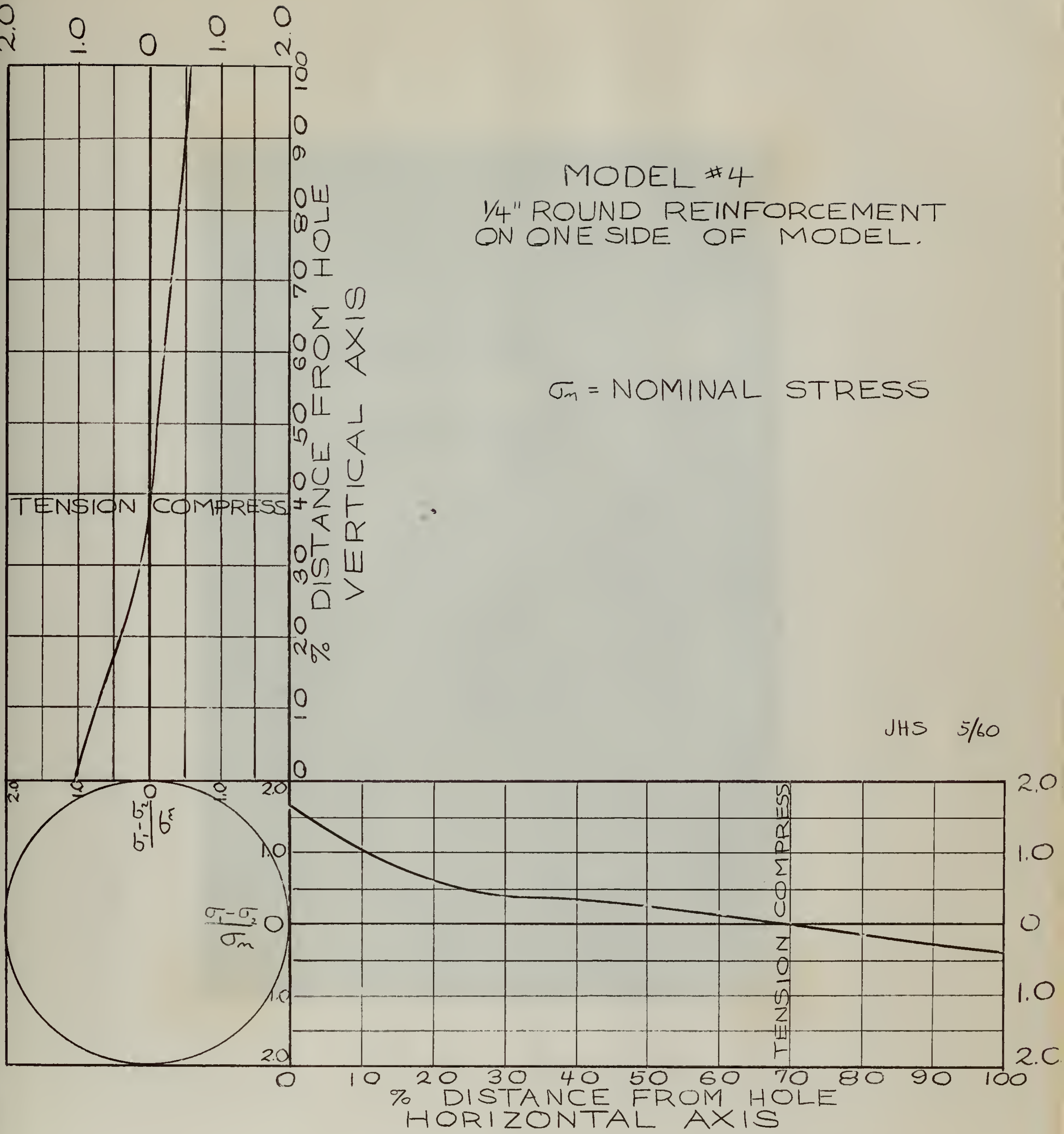

MODEL #4
1/4" ROUND REINFORCEMENT
ON ONE SIDE OF MODEL.

σ_m = NOMINAL STRESS

JHS 5/60

$(\sigma_1-\sigma_2)/\sigma_m$ AS A FUNCTION OF DISTANCE

FIGURE IX. MODEL #4

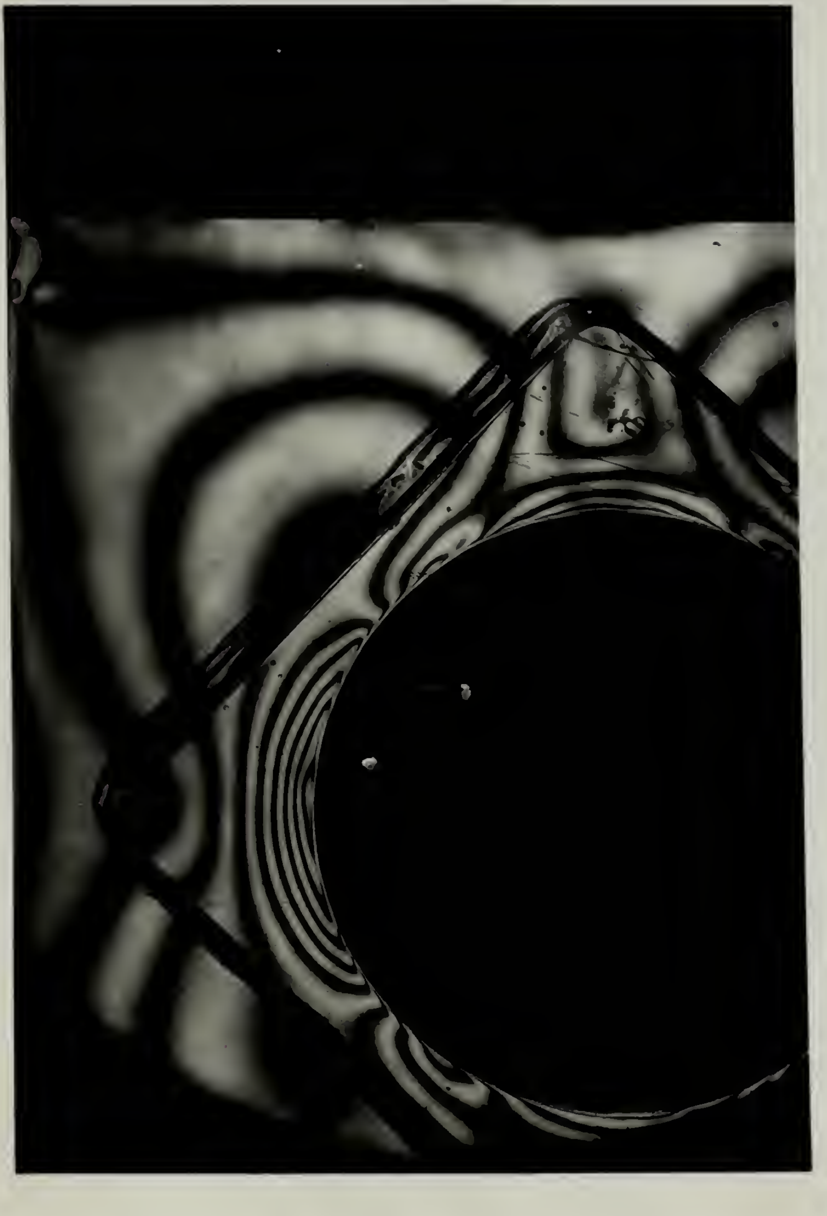

FIGURE X. Plate with 1/8" Square Reinforcement Cemented to both Sides

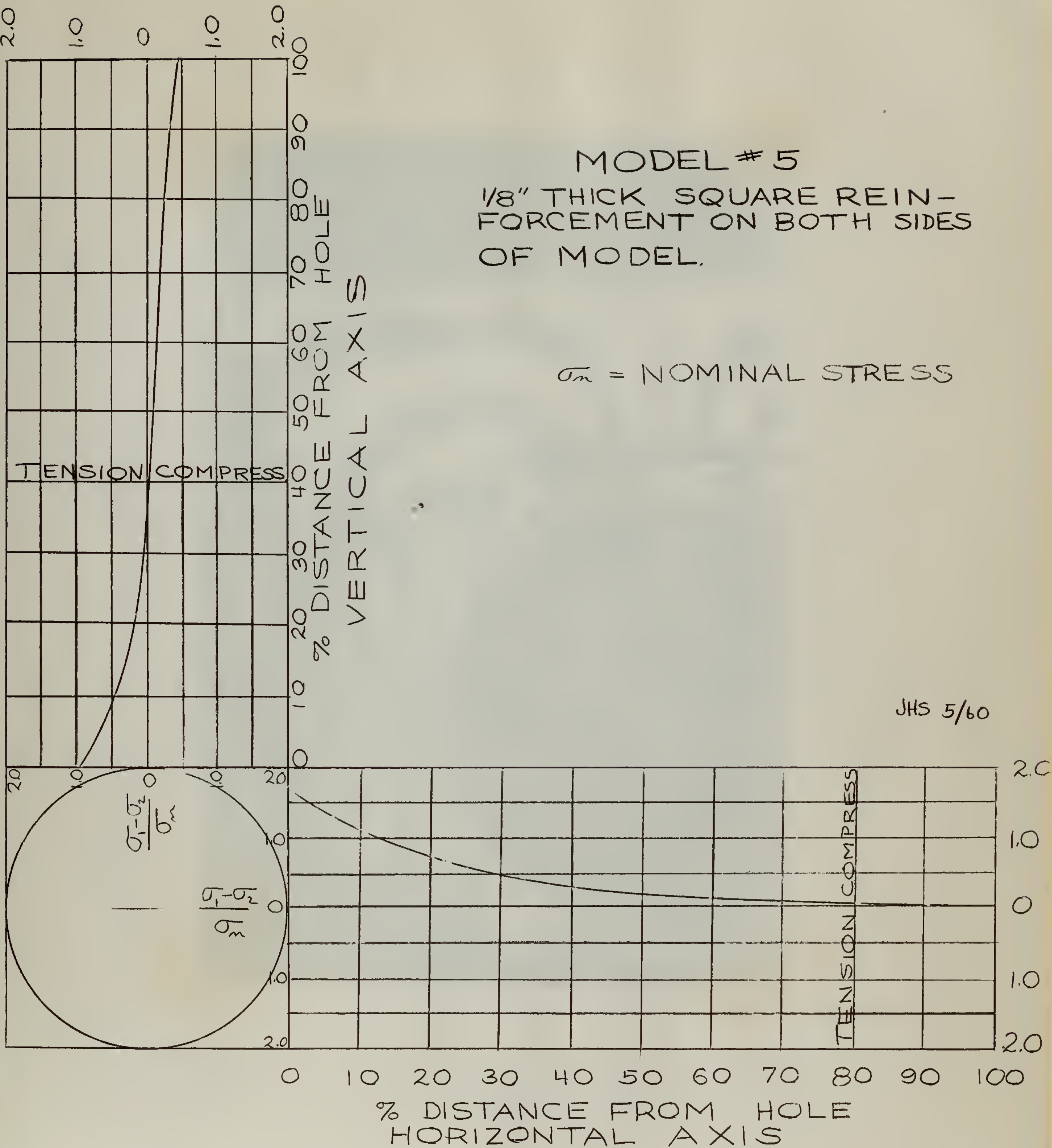

MODEL #5

1/8" THICK SQUARE REINFORCEMENT ON BOTH SIDES OF MODEL.

σ_n = NOMINAL STRESS

JHS 5/60

$(\sigma_1-\sigma_2)/\sigma_n$ AS A FUNCTION OF DISTANCE

FIGURE XI . MODEL #5.

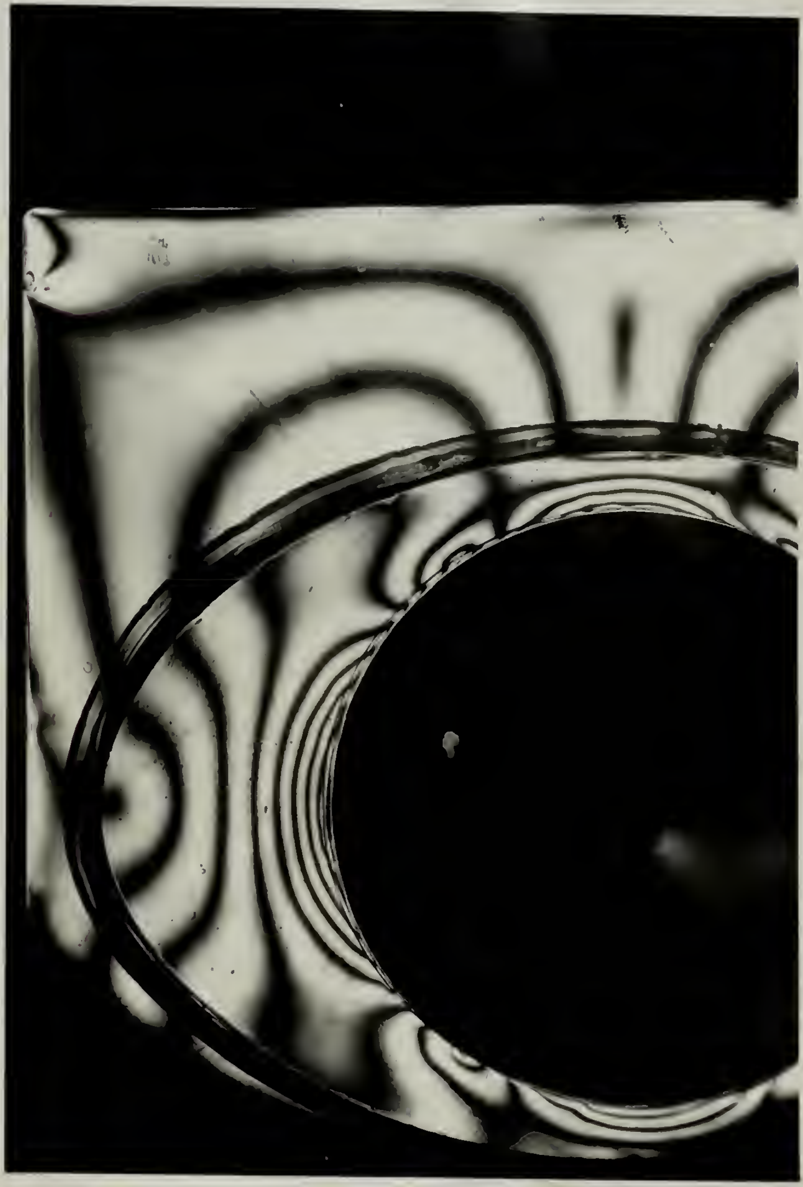

FIGURE XII. Plate with 1/8" elliptical Reinforcement Cemented to both Sides with Major Axis Parallel to Loaded Edges

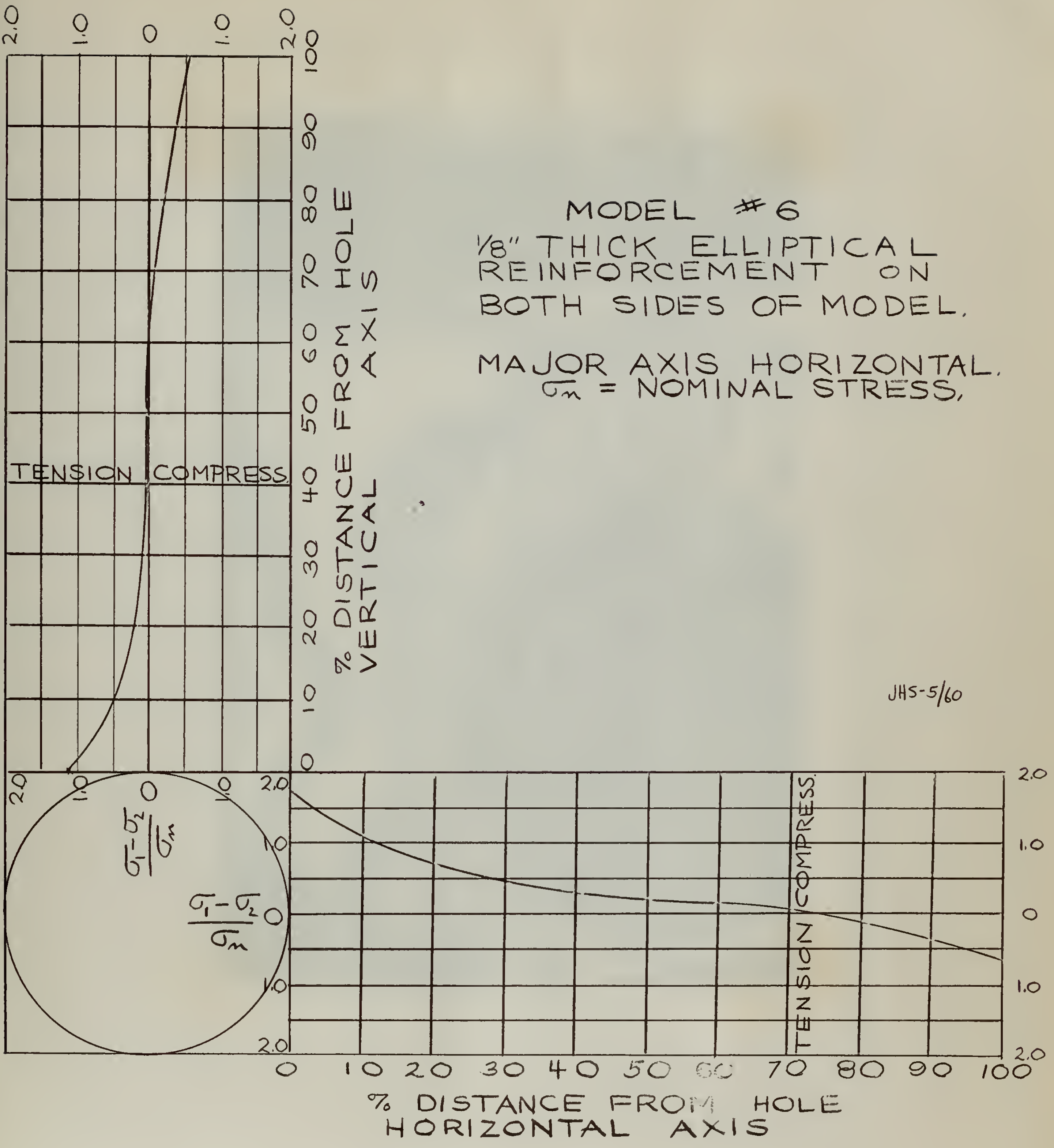

MODEL #6
1/8" THICK ELLIPTICAL
REINFORCEMENT ON
BOTH SIDES OF MODEL.

MAJOR AXIS HORIZONTAL.
σ_m = NOMINAL STRESS.

JHS-5/60

$(\sigma_1 - \sigma_2)/\sigma_m$ AS A FUNCTION OF DISTANCE

FIGURE XIII. MODEL #6.

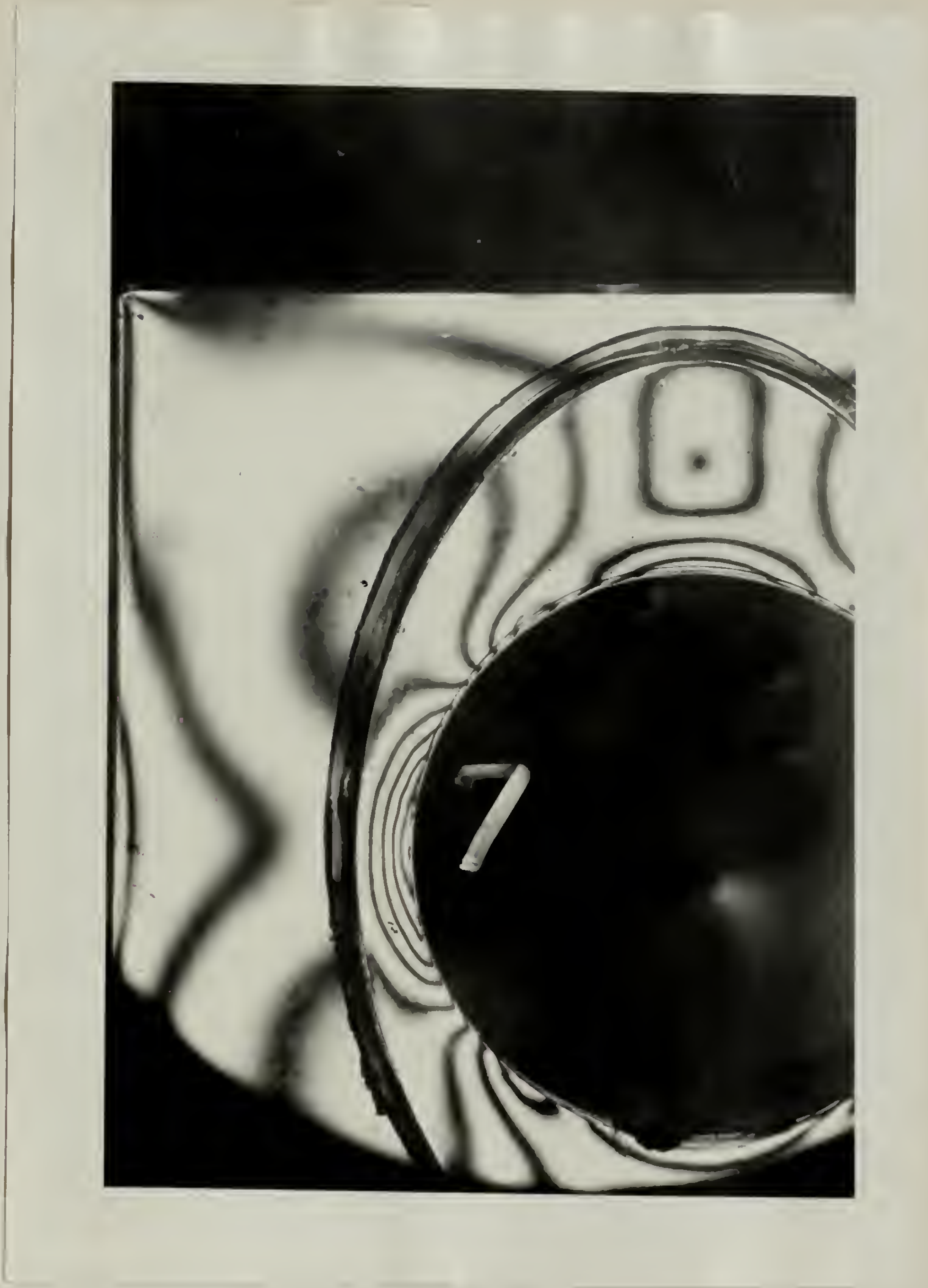

FIGURE XIV. Plate with 1/8" Elliptical Reinforcement Cemented to both Sides with Major Axis Perpendicular to the Loaded Edges

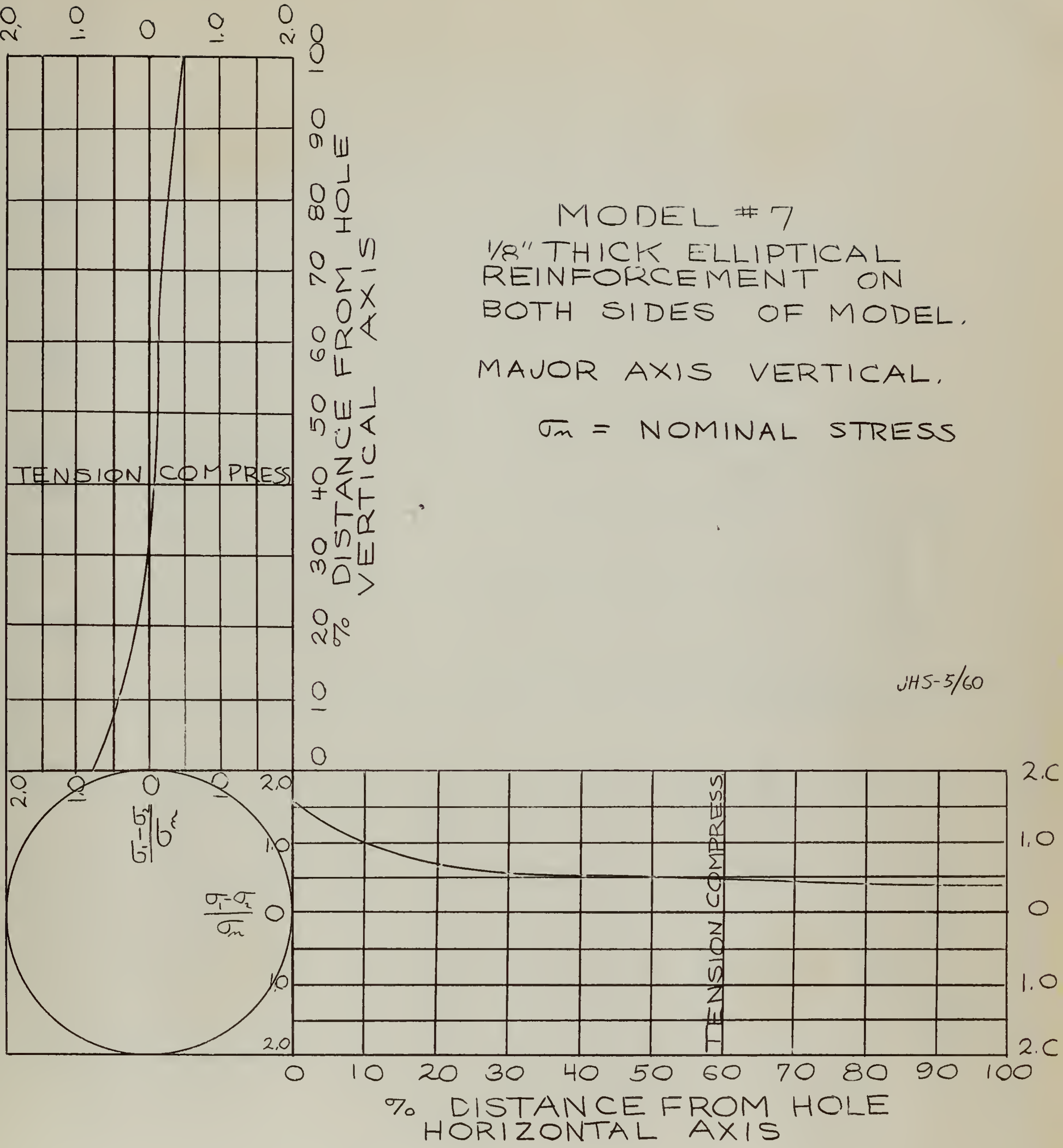

MODEL #7

1/8" THICK ELLIPTICAL REINFORCEMENT ON BOTH SIDES OF MODEL.

MAJOR AXIS VERTICAL.

σ_n = NOMINAL STRESS

JHS-5/60

$(\sigma_1-\sigma_2)/\sigma_n$ AS A FUNCTION OF DISTANCE

FIGURE XV. MODEL #7.

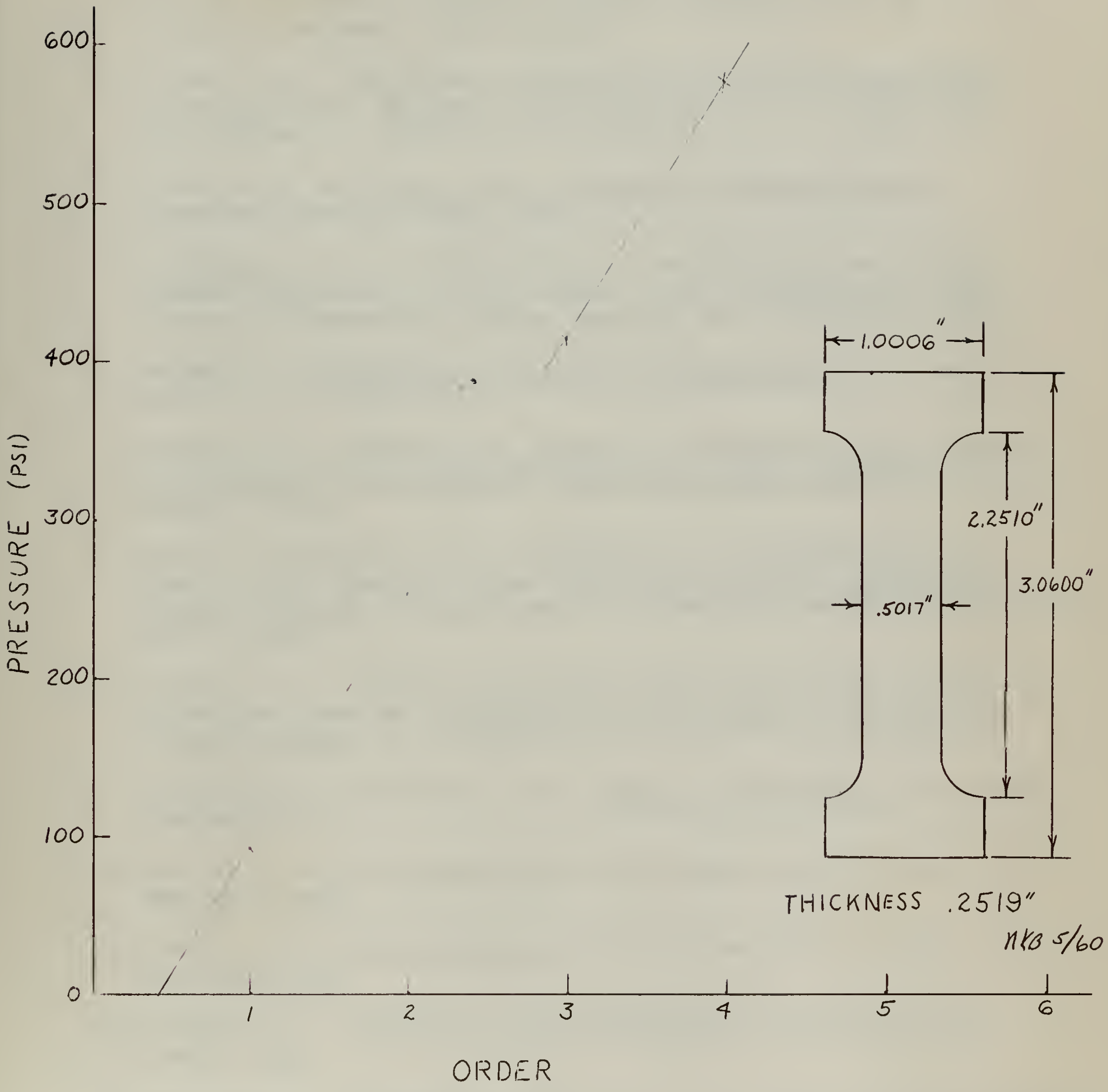

FIGURE XVI. DETERMINATION OF FRINGE CONSTANT

G. LITERATURE CITATIONS

1. Leven, M. M. and Wahl, A. M., "Three-Dimensional Photoelasticity and its Application in Machine Design," American Society of Mechanical Engineers Paper #57-A-87.

2. Frocht, M. M., "The Growth and Present State of Three-Dimensional Photoelasticity", Applied Mechanics Reviews, Vol. 5, August 1952, pp. 337-340.

3. Coker, E. G. and Filon, L.N.G., Treatise on Photoelasticity, Cambridge University Press, 1931.

4. Coolidge, D. J., "An Investigation of the Mechanical and Stress-Optical Properties of Columbia Resin, CR-39", Proceedings of the Society for Experimental Stress Analysis, Vol. VI, Number 1, 1948.

5. Hetenyi, M., Handbook of Experimental Stress Analysis, John Wiley and Sons, New York, 1950.

6. Mantle, J. B., "Photoelastic Analysis of Reinforced Stress Raisers", Proceedings of the Society for Experimental Stress Analysis, Vol. XI, Number 2, 1954.

7. Levy, S., McPherson, A. E., and Smith, F. C., "Reinforcement of a Small Circular Hole in a Plane Sheet Under Tension," Journal of Applied Mechanics (Transactions of the Society of Mechanical Engineers), Vol. 15, 1948.

8. Mindlin, R. D., "Stress Distribution Around a Hole Near the Edge of a Plate Under Tension," Proceedings of the Society for Experimental Stress Analysis, Vol. V, 1948.

9. Timoshenko, S. and Goodier, J. N., Theory of Elasticity, McGraw-Hill, New York, 1951.

10. Frocht, M. M., Photo-Elasticity, Vol. I, John Wiley and Sons, New York, 1949.

11. Frocht, M. M., Photo-Elasticity, Vol. II, John Wiley and Sons, New York, 1948.

12. Heywood, R. B., Designing by Photo-Elasticity, Chapman and Hall, London, 1952.

13. Timoshenko, S., Strength of Materials, D. Van Nostrand Co.,New York,1956.

14. Wahl, A. M., "Stress Concentrations Produced by Holes and Notches," Product Engineering, March, 1934.

15. Frocht, M. M. and Leven, M. M., "On the State of Stress in Thick Bars," Journal of Applied Physics, Vol. 13, May, 1942.

16. Solakian, A. G., "Photoelastic Models with Cemented Elements", Photoelastic Journal, Vol. I, Number 1, January 1938

17. Frocht, M. M., "Factors of Stress Concentration Photoelastically Determined", Transactions of the American Society of Mechanical Engineers, Vol. 57, 1935.

18. Taylor, C. E. and Schweiker, J. W., "A Three-Dimensional Photoelastic Investigation of the Stresses Near a Reinforced Opening in a Reactor Pressure Vessel", Proceedings of the Society for Experimental Stress Analysis, Vol. XVII, Number I, 1959.

thesB424
Photoelastic analysis of reinforced circ
3 2768 002 13740 8
DUDLEY KNOX LIBRARY